

## ANALYSIS OF FORMATION DAMAGE CAUSED BY OIL-BASED MUD ON BEREA SANDSTONE USING SEM

ISSHAM ISMAIL<sup>1</sup> & JAGDEVE BABU<sup>2</sup>

**Abstract.** The objective of this experiment is to investigate the damage caused by oil-based mud on Berea sandstone using Scanning Electron Microscope (SEM). Laboratory experiment had been carried out using synthetic oil-based mud (Sarapar 147) at various differential pressures exerted on the core under dynamic conditions. The discussion of this research results were based on the damage ratio and visual observation of exposed samples using SEM. The damage ratios of the damaged core samples were found to decrease when the differential pressures were increased. These results were confirmed with SEM images. The SEM images and damage ratios also revealed that when samples were positioned at an angle of 180° (horizontal), they experienced higher particles plugging compared to samples positioned at an angle of 90° (vertical).

**Keywords:** Oil-based mud, formation damage, damage ratio, Berea sandstone, SEM

**Abstrak.** Objektif ujikaji ini adalah untuk mengkaji kerosakan yang dialami oleh batu pasir Berea berikutan penggunaan lumpur dasar minyak, dengan menggunakan Mikroskop Elektron Imbasan (SEM – *Scanning Electron Microscope*). Ujikaji dilakukan di makmal menggunakan lumpur dasar minyak sintetik (Sarapar 147) yang beroperasi dalam keadaan dinamik dengan tekanan pembezaan yang berbeza. Keputusan ujikaji dibincang berdasarkan nisbah kerosakan dan analisis secara visual imej SEM sampel teras yang terdedah kepada lumpur. Nisbah kerosakan yang dialami oleh sampel teras rosak didapati berkurangan apabila tekanan pembezaan meningkat. Imej SEM juga didapati memberikan keputusan yang sama. Imej SEM dan nisbah kerosakan turut membuktikan bahawa sampel yang dipasang pada sudut 180° (mendatar) mengalami penyumbatan partikel yang lebih ketara berbanding sampel yang dipasang pada sudut 90° (tegak).

**Kata kunci:** Lumpur dasar minyak, kerosakan formasi, nisbah kerosakan, batu pasir Berea, SEM

### 1.0 INTRODUCTION

Formation damage can be caused by either a simple or complex process involving any of the phases of producing oil or gas. The dynamics of drilling alone is so great that this process is capable of altering adversely the rock's ability to flow fluids [1]. Formation damage is attributed primarily from two main sources, namely particles plugging and filtrate invasion from drilling fluids [2]. Therefore, to prevent permeability damage effectively, the damage mechanisms should be identified in the first place.

<sup>1</sup> Faculty of Chemical and Natural Resources Engineering, Universiti Teknologi Malaysia, 81310 Skudai, Johor Darul Takzim, Malaysia.

<sup>2</sup> Schlumberger Asia Solutions Center, 18<sup>th</sup> Floor, East Wing, Rohas Perkasa, No. 8, Jalan Perak, 50450 Kuala Lumpur.

The damaging solids may come directly from the fluid system or the formation itself. Invasion of drilling fluid solids into the formation during drilling can eventually cause permeability impairment and thus reduction in well productivity. This is due to the particles plugging in pore spaces, which in turn causes an obstruction for the oil droplets from moving around the wellbore. Particles plugging is most severe at the wellbore face [3].

In this study, the particles plugging mechanism was studied with the assistance of Scanning Electron Microscope (SEM) [4]. The SEM was used to provide qualitative information about the pore geometry and to study the damage mechanism at microscopic level [5]. An Energy Dispersive X-ray (EDX) was also used to provide surface qualitative information of chemical elements and minerals found on the surface of the core samples [6,7].

## 2.0 MATERIALS AND EXPERIMENTAL SYSTEM

### 2.1 Materials

The oil-based mud was prepared using Sarapar 147 that was supplied by Shell. Sarapar is a light synthetic mineral oil that was used as the base fluid in this drilling mud preparation. Kota Minerals and Chemicals (M) Sdn. Bhd. (KMC), a drilling mud service company based in Kemaman, Terengganu, supplied the drilling mud additives. The oil-based mud was prepared as per field formulation suggested by the ExxonMobil Production Malaysia Inc. (EMPMI), as shown in Table 1. Table 2 shows the functions of the respective mud additives used in the mud system.

Berea sandstone cores with dimensions of 6 inches (15.24 cm) in length and 2 inches (5.08 cm) in diameter were used in this study to evaluate the damage induced

**Table 1** The formulation of oil-based mud

Composition	Quantity
Sarapar 147 (ml)	242.0
Versamul (ppb)	5.0
Versacoat (ppb)	2.0
Lime (ppb)	5.0
Drill water (ml)	60.6
Calcium Chloride, CaCl (ppb)	15.0
Visplus (ppb)	6.0
Versatrol (ppb)	5.0
Barite, Ba <sub>2</sub> SO <sub>4</sub> (ppb)	170.0

**Table 2** The functions of the mud additives

Additives	Function(s)
Versamul	(1) Multi-purpose emulsifier. (2) Gelling agent. (3) Fluid stabilizing additives in a non-toxic base.
Versacoat	(1) Secondary emulsifier.
Lime	(1) To control pH.
Calcium chloride	(1) Osmotic control to stabilize reactive clay formation.
Visplus	(1) Emulsifying agent.
Versatrol	(1) To reduce fluid loss.(2) To control filtration.
Barite	(1) To increase density of mud (weighting agent).

by oil-based mud at various pressure differentials under dynamic conditions. In fact, Berea sandstone has been used for decades as test samples in the formation damage studies. It was supplied by Cleveland Quarries, USA, and has permeability and porosity of 100–200 md ( $986.9\text{--}1973.8 \times 10^{-4} \mu\text{m}^2$ ) and 20% respectively.

## 2.2 EXPERIMENTAL SYSTEM

This research study comprises of two processes:

- (1) Induce damage to the core samples using oil-based mud via the custom fabricated rig.
- (2) Sample preparation for SEM and EDX analysis.

### 2.2.1 Process of Damaging the Core Samples

The experimental work was set up to study two different variables, namely the differential pressure and core position (angle). The ranges of the two experimental variables tested were:

- (1) Differential pressure: 100–250 psi (689.5–1723.7 kPa).
- (2) Angle: 90° (vertical) and 180° (horizontal).

Oil-based mud was prepared in the Drilling Laboratory of Universiti Teknologi Malaysia using conventional lab equipments. After the mud was prepared, mud rheological properties were measured using standard equipments, namely mud balance, rheometer, and High Pressure High Temperature (HPHT) filter press as recommended by the American Petroleum Institute (API) [8].

Eight Berea sandstone core samples were used in this experiment. Prior to the test, these core samples were saturated with Sarapar 147.

The severity of damage experienced by the core samples after being exposed to oil-based mud was evaluated according to the measurements of their initial permeabilities,  $k_i$ , and damaged permeabilities,  $k_d$ . The experimental apparatus, as shown in Figure 1, was used to measure the initial and damaged permeability of the core samples.

Nitrogen gas was used to force Sarapar 147 from its container to flow through the core samples. The volume of Sarapar 147, which was collected as filtrate, was used to calculate the flow rate using the following equation:

$$Q = V/t \quad (1)$$

The calculated flow rate was then substituted into the Darcy's equation to calculate the permeability of each of those core samples:

$$k = (Q\mu L)/(A\Delta P) \quad (2)$$

After measuring the initial permeability, the core sample was placed in the core holder of the formation damage rig, as shown in Figure 2. The core was then exposed to the drilling mud at the predetermined differential pressures, and was conducted at vertical and horizontal positions, to simulate the vertical and horizontal wells respectively. The core was exposed to the mud for 30 minutes and filtrate was collected for the same period of time. After the damaging process, the core sample was removed from the formation damage rig and placed in the permeability measurement apparatus (Figure 1) to measure the damaged permeability of the core. The damaged permeability of the core sample was then computed using Equation (2). It is meaningless to directly use the damaged permeability derived from the Darcy's equation when comparing

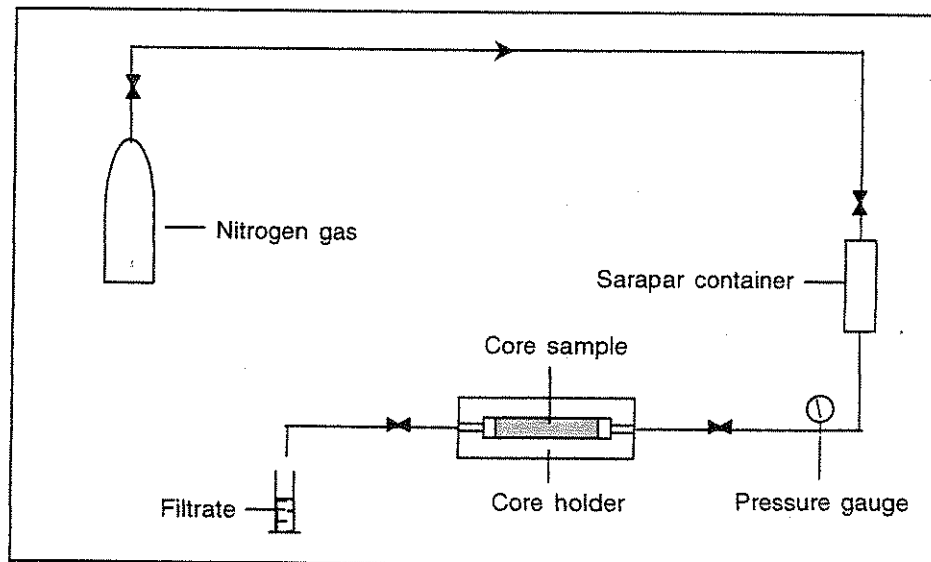


**Figure 1** Schematic of the permeability measurement apparatus

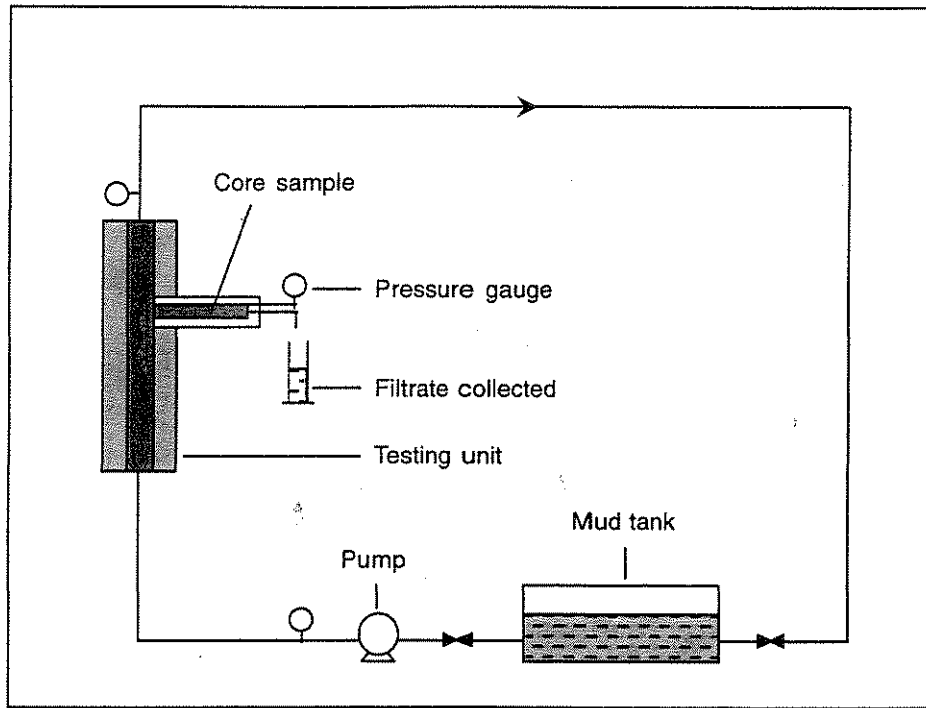


**Figure 2** Schematic of the formation damage rig

the severity of damage experienced by those core samples, as they have different initial permeabilities. Therefore, the Damage Ratio (DR) was introduced in this study, and it was calculated by taking the ratio of the permeability of the core after damage,  $k_d$  to the initial permeability of the core before damage,  $k_i$ . Mathematically, DR, in percentage, can be written as:

$$DR = (k_d/k_i) \times 100\% \quad (3)$$

### 2.2.2 Sample Preparation for SEM and EDX Analysis

The core samples that were damaged in the process mentioned previously, would develop a layer of mud cake on their surface and had to be cleaned thoroughly. A thin section of the damaged sample was then cut at a thickness of two millimeters from the top. Samples were then labeled and trimmed to the recommended size for SEM analysis. These samples were then dried and rockflour was removed from the them, as rockflour might cause disturbance during the analysis process. Thereafter, these samples were coated with carbon and ready to be viewed under the electron microscope [4]. The EDX was done on a clean core, in which three grams of fine powdered (20 microns) was prepared by finely grinding the sample [5,7]. Detailed standard procedures of conducting the SEM and EDX are shown in References [9,10], respectively.

### 3.0 RESULTS AND DISCUSSION

Generally, the data obtained and discussed can be divided into three main parts, namely:

- (1) Petrography analysis on a clean core.
- (2) Effects of various differential pressures on formation damage.
- (3) Comparison of formation damage in vertical and horizontal core samples.

#### 3.1 Petrography Analysis on a Clean Core

The SEM image of a clean Berea sandstone core sample was analyzed to understand the grain structure and pore structure. The SEM image enabled a three dimensional view of the core sample at a microscopic level. The SEM image revealed that the grains ranged from subrounded to subangular (Figure 3). It is also noted that the pore sizes ranged from 65  $\mu\text{m}$  to 84  $\mu\text{m}$ . The EDX analysis revealed that the Berea sandstone core sample used was clean with no traces of clay minerals present, as confirmed by the supplier of the Berea sandstone (Table 3). The absence of clay minerals in the core samples means that when a core sample is exposed to drilling mud, the damage experienced is solely due to the particles plugging – free from the effect of clay swelling – otherwise, the damage results will be difficult to analyze.

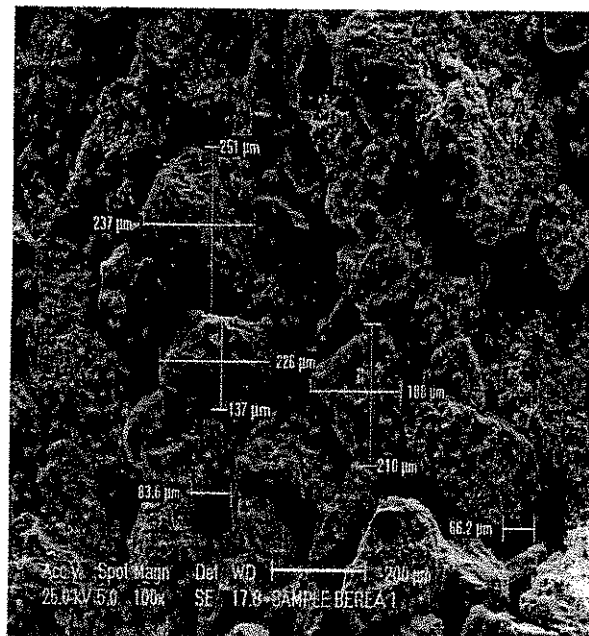


**Figure 3** SEM image of a clean core sample at 100X magnification showing the grain sizes

**Table 3** Minerals content of a Berea sandstone core sample

SSNNNN	Compound Name	Formula	Y Scale	dx by	Wavelength	System	a	b	c	alpha	beta	gamma
DIF	BEREA-1A	Berea-1a.dif	100.00	1.	1.54056							
85-0335(C)	Quartz low	SiO2	50.00	1.	1.54056	Hexagonal	4.91340	4.91340	5.40520	90.000	90.000	120.000
78-1252(C)	Quartz alpha syn	SiO2	50.00	1.	1.54056	Hexagonal	4.91920	4.91920	5.40500	90.000	90.000	120.000
87-2096(C)	Quartz	SiO2	50.00	1.	1.54056	Hexagonal	4.91270	4.91270	5.40450	90.000	90.000	120.000
85-0795(C)	Quartz	SiO2	50.00	1.	1.54056	Hexagonal	4.91080	4.91080	5.40280	90.000	90.000	120.000
85-0798(C)	Quartz	SiO2	50.00	1.	1.54056	Hexagonal	4.91400	4.91400	5.40500	90.000	90.000	120.000
85-0796(C)	Quartz	SiO2	50.00	1.	1.54056	Hexagonal	4.91180	4.91180	5.40340	90.000	90.000	120.000
85-0797(C)	Quartz	SiO2	50.00	1.	1.54056	Hexagonal	4.91410	4.91410	5.40440	90.000	90.000	120.000
79-1906(C)	Quartz	SiO2	50.00	1.	1.54056	Hexagonal	4.91340	4.91340	5.40520	90.000	90.000	120.000
85-0930(C)	Quartz	SiO2	50.00	1.	1.54056	Hexagonal	4.91100	4.91100	5.40700	90.000	90.000	120.000
79-1910(C)	Quartz	SiO2	50.00	1.	1.54056	Hexagonal	4.91400	4.91400	5.40600	90.000	90.000	120.000
85-1053(C)	Quartz synthetic	SiO2	50.00	1.	1.54056	Hexagonal	4.91280	4.91280	5.40420	90.000	90.000	120.000
86-1560(C)	Quartz low	SiO2	50.00	1.	1.54056	Hexagonal	4.91600	4.91600	5.40540	90.000	90.000	120.000
86-1630(C)	Quartz low	SiO2	50.00	1.	1.54056	Hexagonal	4.91410	4.91410	5.40600	90.000	90.000	120.000
85-0695(C)	Silicon Oxide	SiO2	50.00	1.	1.54056	Hexagonal	4.91340	4.91340	5.40520	90.000	90.000	120.000
85-0504(C)	Quartz	SiO2	50.00	1.	1.54056	Hexagonal	4.91280	4.91280	5.40420	90.000	90.000	120.000
78-2315(C)	Quartz	SiO2	50.00	1.	1.54056	Hexagonal	4.91239	4.91239	5.40385	90.000	90.000	120.000
77-1060(C)	Silicon Oxide	SiO2	50.00	1.	1.54056	Tridinic	4.91600	4.91700	5.40700	90.000	90.000	120.000
86-2237(C)	Quartz low	SiO2	50.00	1.	1.54056	Hexagonal	4.91300	4.91300	5.40400	90.000	90.000	120.000
85-0457(C)	Silicon Oxide	SiO2	50.00	1.	1.54056	Hexagonal	4.92100	4.92100	5.40000	90.000	90.000	120.000
46-1045(*)	Quartz syn	SiO2	50.00	1.	1.54056	Hexagonal	4.91344	4.91344	5.40524	90.000	90.000	120.000
83-0539(C)	Quartz	SiO2	50.00	1.	1.54056	Hexagonal	4.92100	4.92100	5.41630	90.000	90.000	120.000
85-1054(C)	Quartz alpha	SiO2	50.00	1.	1.54056	Hexagonal	4.90390	4.90390	5.39430	90.000	90.000	120.000
86-1629(C)	Quartz low	SiO2	50.00	1.	1.54056	Hexagonal	4.90300	4.90300	5.39990	90.000	90.000	120.000
86-1628(C)	Quartz low	SiO2	50.00	1.	1.54056	Hexagonal	4.90210	4.90210	5.39970	90.000	90.000	120.000
84-0853(C)	Aluminum Phosphate	AlPO4	50.00	1.	1.54056	Hexagonal	4.92700	4.92700	10.91800	90.000	90.000	120.000
85-0865(C)	Quartz alpha	SiO2	50.00	1.	1.54056	Hexagonal	4.90000	4.90000	5.40000	90.000	90.000	120.000
85-0794(C)	Berlinite, syn	AlPO4	50.00	1.	1.54056	Hexagonal	4.89000	4.89000	10.86900	90.000	90.000	120.000
85-0794(C)	Silicon Oxide	SiO2	50.00	1.	1.54056	Hexagonal	4.90000	4.90000	5.39000	90.000	90.000	120.000
26-1077(C)	Carbon	C	50.00	1.	1.54056	Hexagonal	2.456	2.45600	16.740	90.000	90.000	120.000
85-1780(C)	Quartz	SiO2	50.00	1.	1.54056	Hexagonal	4.89000	4.89000	5.49000	90.000	90.000	120.000
26-1080(C)	Carbon	C	50.00	1.	1.54056	Hexagonal	2.456	2.45600	13.392	90.000	90.000	120.000
26-1076(C)	Carbon	C	50.00	1.	1.54056	Hexagonal	2.456	2.45600	20.088	90.000	90.000	120.000
76-0225(C)	Berlinite, syn	AlPO4	50.00	1.	1.54056	Hexagonal	4.94100	4.94100	10.94000	90.000	90.000	90.000
76-0227(C)	Berlinite, syn	AlPO4	50.00	1.	1.54056	Hexagonal	4.94100	4.94100	10.94000	90.000	90.000	120.000
84-0854(C)	Aluminum Phosphate	AlPO4	50.00	1.	1.54056	Hexagonal	4.95000	4.95000	10.94800	90.000	90.000	120.000
85-1721(C)	Berlinite, syn	AlPO4	50.00	1.	1.54056	Hexagonal	4.94230	4.94230	10.94460	90.000	90.000	120.000
75-1072(C)	Berlinite, syn	AlPO4	50.00	1.	1.54056	Hexagonal	4.94230	4.94230	10.94460	90.000	90.000	120.000

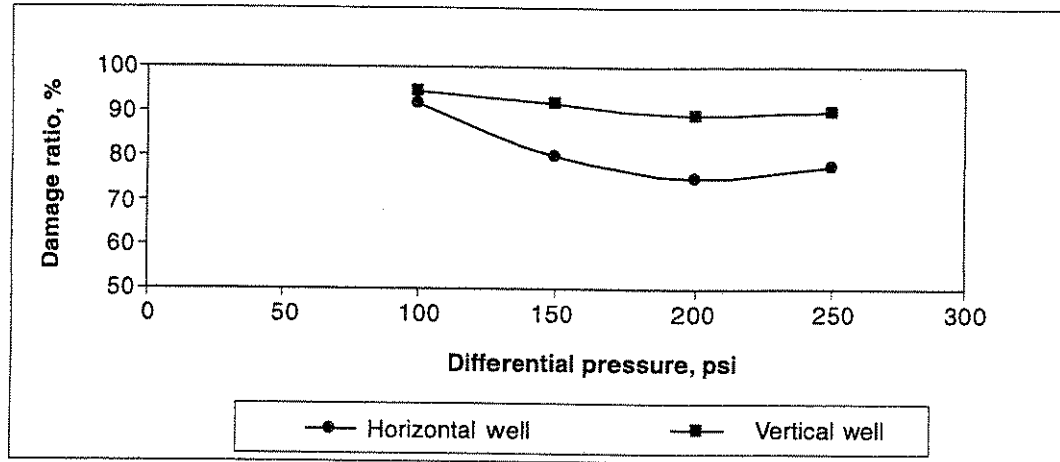


**Figure 4** Damage ratio for vertical and horizontal wells

### 3.2 Effects of Various Differential Pressures on Formation Damage

The differential pressures used in this experiment was in the range of 100–250 psi (689.5–1723.7 kPa), with annular velocity and temperature being kept constant at 60 ft/min (0.31 m/s) and 176°F (80°C) respectively. Oil-based mud was flowed in the system for 30 minutes and the rheological properties of the mud were re-tested at the end of each run. In this research study, the Berea sandstone core samples were installed horizontally and vertically to simulate horizontal and vertical wells.

This research study revealed that the severity of damage to the core by drilling mud was found to be inversely proportional to the damage ratio. Results show that higher differential pressures caused severe damages, as shown in Figures 4.

At higher differential pressures, the migration of solid particles into core samples increased due to the increase in driving force acting on the respective particles. Total solid migration into the core samples was proportional to the differential pressures. Greater solid invasion caused severe blockage of pore throats, thus it induced greater reduction in permeability of the core sample.

The damage experienced by the core samples was confirmed by the SEM images, as it revealed an increase on the density of particles plugging into the core samples when the differential pressures increased. Figures 5 and 6 clearly show the Berea sandstone core samples that were severely plugged by particles from oil-based mud.

### 3.3 Comparison of Formation Damage in Horizontal and Vertical Core Samples

The experimental results revealed that horizontal core samples experienced more damage compared to vertical core samples (Figure 4). A comparison of SEM images

revealed that core samples that were positioned vertically, experienced lesser particles plugging compared to core samples that were positioned horizontally.

When positioned vertically, mud invasion into the Berea sandstone core samples was in a cylindrical pattern. On the other hand, in the horizontal core samples, due to the frequent anisotropy condition, the mud invasion pattern was elliptical. The elliptical invasion pattern was capable in forcing more mud particles into the core samples positioned horizontally, as compared to cylindrical pattern on vertical core samples [7]. Thus, this phenomenon causes horizontal well to experience more damage than vertical well. The SEM images proved that particles plugging was more critical in samples positioned horizontally, as shown in Figures 5 and 6. The SEM images clearly show the relative difference between samples positioned horizontally and vertically, in which samples positioned horizontally had less pore openings after the experiment was conducted.

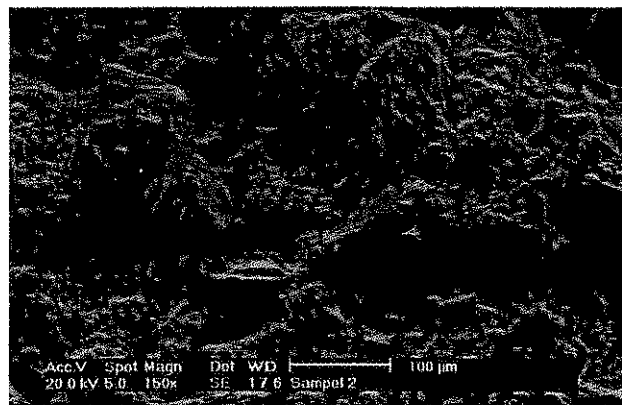


**Figure 5** SEM image of a Berea sandstone core sample, damaged at 150 psi (1034.2 kPa) at an angle of 180°

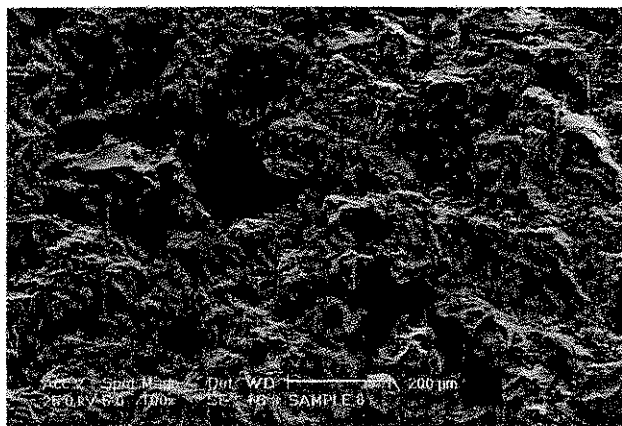


**Figure 6** SEM image of a Berea sandstone core sample, damaged at 150 psi (1034.2 kPa) at an angle of 90°

Besides that, when the testing unit of the formation damage rig was positioned horizontally, simulating a horizontal well due to the gravity effect, mud particles tend to move towards the bottom of the unit. This caused more particles to be forced into the horizontal core samples, which led to severe damage. This in turn also led to the forming of less permeable mud cake and lower filtrate loss in horizontal core samples for all differential pressures, as compared to core samples positioned vertically (Table 4).

**Table 4** Filtrate loss at the end of 30 minutes

Differential pressure (psi)	Horizontal core sample (ml)	Vertical core sample (ml)
100	1.8	2.4
150	2.1	2.8
200	2.6	3.8
250	2.9	3.9

#### 4.0 CONCLUSION

The following conclusions were derived from this research study:

- (1) The SEM images qualitatively revealed that higher differential pressures caused severe formation damage. The SEM result was found to be in good agreement with the damage ratios. Generally, at higher differential pressures, the migration of solid particles into core samples becomes more critical. Consequently, it reduces the damage ratio of the Berea sandstone core samples.
- (2) Horizontal core samples experienced more damage compared to vertical core samples due to the anisotropy flow and gravity effect in the mud flow pattern.
- (3) The primary damage mechanism in all samples was due to particles plugging. Generally, the relative size of pore openings and plugging materials determine the amount of particles plugging into core samples.
- (4) EDX analysis proved that the Berea sandstone core samples did not contain any clay minerals, thus damage experienced by core samples was solely due to particles plugging.
- (5) Filtrate loss was found to be lower in horizontal core samples due to the presence of less permeable mud cakes.

#### NOMENCLATURE

- $A$  : Area, in<sup>2</sup>  
 $DR$  : Damage Ratio, dimensionless  
 $EDX$  : Energy Dispersive X-Ray

$k$	: Permeability, Darcy
$k_d$	: Damaged permeability, Darcy
$k_i$	: Initial permeability, Darcy
$L$	: Core length, inches
$Q$	: Flow rate, cc/s
SEM	: Scanning Electron Microscope
$t$	: Time, sec.
$V$	: Volume, cc
$\Delta P$	: Differential pressure, psi
$\mu$	: viscosity, cP

### ACKNOWLEDGEMENT

The authors would like to thank the Malaysian Government for the financial assistance given via the IRPA grant (Vot: 72232).

### REFERENCES

- [1] Byrne, M. T., I. S. C. Spark, I. T. M. Patey., and A. J. Twynam. 2000. A Laboratory Drilling Mud Overbalance Formation Damage Study Utilizing Cryogenic SEM techniques. *SPE International Symposium on Formation Damage Control* (SPE 58738). Lafayette. Louisiana. 23-24 February.
- [2] Allen, T. O., and A. P. Roberts. 1993. *Production Operation: Well Completions, Workover and Stimulation*. 4<sup>th</sup> ed. Oklahoma: Oil & Gas Consultants.
- [3] Krueger, R. F. 1986. An Overview of Formation Damage and Well Productivity in Oilfield Operations. *J. Pet. Tech.* February. 131-152.
- [4] Spark, I. S. C., and I. T. M. Patey. 1994. The Use of SEM and Cryogenic SEM Analysis in Formation Damage Flood Test Studies. *5<sup>th</sup> International Oil Field Chemicals Symposium*. Geilo, Norway. 20-23 Mac.
- [5] Pittman, E. D., and J. B. Thomas. 1979. Some Applications of Scanning Electron Microscopy to the Study of Reservoir Rock. *SPE 53<sup>rd</sup> Annual Fall Technical Conference and Exhibition* (SPE 7550). Houston. 1-3 October.
- [6] Marshall, D. S. 1997. Development of a Recommended Practice for Formation Damage Testing. *SPE European Formation Damage Conference* (SPE 38154). The Netherlands. 2-3 June.
- [7] Bennion, D. B., F. B. Thomas., and R. F. Bietz. 1996. Formation Damage and Horizontal Wells – A Productivity Killer? *International Conference on Horizontal Well Technology* (SPE 37138). Calgary. Alberta. Canada. 18-20 November.
- [8] American Petroleum Institute. 1990. *API Recommended Practice Standard Procedure for Field Testing Oil-Based Drilling Fluids*. API RP 13B-2.
- [9] Philips. 1990. Scanning Electron Microscope XL Series. *Operating Instruction*. Amsterdam: Philips Analytical, Electron Optics, Application Laboratory.
- [10] Philips. 1990. EDX Microanalysis. *Operating Instruction*. Amsterdam: Philips Analytical, Electron Optics, Application Laboratory.

**CONVERSION FACTOR**

$(^{\circ}\text{F} - 32)/1.8$		=	$^{\circ}\text{C}$
$\text{bbl} \times 1.589\,873$	E - 01	=	$\text{m}^3$
$\text{cP} \times 1.0$	E - 03	=	$\text{Pa.s}$
$\text{ft} \times 3.048^*$	E - 01	=	$\text{m}$
$\text{gal} \times 3.785\,412$	E - 03	=	$\text{m}^3$
$\text{in.} \times 2.54^*$	E + 00	=	$\text{cm}$
$\text{lbm} \times 4.535\,924$	E - 01	=	$\text{kg}$
$\text{md} \times 9.869233$	E - 04	=	$\mu\text{m}^2$
$\text{ppg} \times 1.198\,264$	E + 02	=	$\text{kg/m}^3$
$\text{psi} \times 6.894\,757$	E + 00	=	$\text{kPa}$

\* Conversion factor is exact.